

Dalton Transactions

An international journal of inorganic chemistry

Accepted Manuscript

This article can be cited before page numbers have been issued, to do this please use: A. Palii, V. Belonovich, D. V. Korchagin, S. M. Aldoshin and B. Tsukerblat, *Dalton Trans.*, 2026, DOI: 10.1039/D6DT00503A.



This is an Accepted Manuscript, which has been through the Royal Society of Chemistry peer review process and has been accepted for publication.

Accepted Manuscripts are published online shortly after acceptance, before technical editing, formatting and proof reading. Using this free service, authors can make their results available to the community, in citable form, before we publish the edited article. We will replace this Accepted Manuscript with the edited and formatted Advance Article as soon as it is available.

You can find more information about Accepted Manuscripts in the [Information for Authors](#).

Please note that technical editing may introduce minor changes to the text and/or graphics, which may alter content. The journal's standard [Terms & Conditions](#) and the [Ethical guidelines](#) still apply. In no event shall the Royal Society of Chemistry be held responsible for any errors or omissions in this Accepted Manuscript or any consequences arising from the use of any information it contains.

Modelling the non-equilibrium low-temperature magnetic cooling effect in Mn_{12} clusters

View Article Online
DOI: 10.1039/D6DT00503A

Andrew Palii,*,¹ Valeria Belonovich,^{1,2} Denis Korchagin,¹ Sergei Aldoshin,¹
Boris Tsukerblat *,³

¹*Federal Research Center of Problems of Chemical Physics and
Medicinal Chemistry of RAS, Chernogolovka, Moscow Region, 142432 RF*

²*Moscow Institute of Physics and Technology, Dolgoprudny,
Moscow Region, 141701, RF*

³*Department of Chemistry, Ben-Gurion University of the Negev,
84105 Beer-Sheva, Israel*

* *Corresponding authors' e-mails: andrew.palii@uv.es; tsuker@bgu.ac.il*

Abstract

Based on the theoretical framework recently developed by some of us, we predict and justify a possibility for the nonequilibrium magnetic cooling effect in Mn_{12} family clusters by considering monocrystalline sample of the prototypical single-molecule magnet $Mn_{12}Ac$ as a representative example. In contrast to the quasi-static processes underlying the conventional magnetocaloric effect (MCE), we address a dynamic regime involving sudden magnetic field quenching. The proposed cooling mechanism is determined by the relaxation kinetics arising after a sudden change in the spin Hamiltonian that generates a nonequilibrium population distribution within the spin subsystem and therefore does not rely on the standard equilibrium entropy cycles. During the subsequent restoration of thermal equilibrium, heat is redistributed between the phonon bath and the spin degrees of freedom. Under the appropriate conditions, this relaxation-driven process results in cooling of the lattice. The central result is that the strong easy-axis magnetic anisotropy associated with a significant magnetization reversal barrier, features typically considered enemies of conventional magnetocaloric cooling, become advantageous in the nonequilibrium regime. These properties enhance both the magnitude of the cooling effect and the practical feasibility of the sudden-quench approach. The study therefore broadens the potential cryogenic applicability of single-molecule magnets by identifying a cooling mechanism that operates precisely in the parameter range where classical magnetocaloric approaches are least efficient.



Abbreviations: SMM-single-molecule magnet, MCE- magnetocaloric effect, RMCE-rotational magnetocaloric effect, $Mn_{12}Ac$ - Mn_{12} -acetate, zero-field splitting-ZFS

1. Introduction

Molecular nanomagnets and single-molecule magnets (SMMs) have garnered significant attention over the past decades, primarily due to their potential applications in high-density data storage and quantum information processing [1-7]. Among them, a famous dodecanuclear manganese cluster $[Mn_{12}O_{12}(CH_3COO)_{16}(H_2O)_4]$, commonly referred to as $Mn_{12}Ac$, represents the prototypical SMM [1,2,4-9]. Numerous Mn_{12} derivatives of general formula $[Mn_{12}O_{12}(RCOO)_{16}(H_2O)_x]Y$ (where Y denotes the solvent molecule) have been synthesized and structurally characterized [1]. Examples include $R=CH_2CH_3$, $x=3$, $Y=4H_2O$ [10,11], $R=CH_2C(CH_3)_2$, $x=4$, $Y=4H_2O$ as well as many other derivatives are presented in Refs [1-3].

Let us first summarize the main structural features of Mn_{12} family [1-3] predetermining their functional properties, which are the subject of this article. The $Mn_{12}Ac$ cluster contains 12 manganese ions surrounded by sixteen acetate groups (Fig. 1). The core comprises a tetrahedron of four Mn^{IV} ions ($s = 3/2$) and an outer ring of eight Mn^{III} ions ($s = 2$), which are linked together by oxo groups and acetate bridging ligands. The crystal of $Mn_{12}Ac$ has tetragonal symmetry (space group $I\bar{4}$) and the dodecanuclear cluster has S_4 symmetry. The crystal structure also includes four solvate water molecules and two CH_3COOH molecules that link the $Mn_{12}Ac$ clusters [1,2]. The eight $s=2$ spins of the Mn^{IV} ions are coupled ferromagnetically as well as four $s=3/2$ spins of the Mn^{IV} ions. Antiferromagnetic exchange interaction between ions with different oxidation states leads to the formation of a ferrimagnetic structure with a total molecular spin of $S = 10$ in the ground state. This molecule exhibits pronounced easy axis-type magnetic anisotropy, which arises primarily from the local anisotropies caused by the Jahn-Teller distortions of the eight $Mn(III)$ sites. The molecular easy axis of magnetization is parallel to the tetragonal c -axis of the crystal lattice and normal to the disk-like core of the molecule. This anisotropy gives rise to a bistable magnetic ground state in which $M_s = +1/2$ and $M_s = -1/2$ substates are separated by a substantial magnetization reversal barrier, which is responsible for the slow relaxation of magnetization at low temperatures. Besides pure scientific interest, $Mn_{12}Ac$ and its derivatives are attractive due to their potential applications in spintronics, quantum computing and ultra-dense data storage devices.



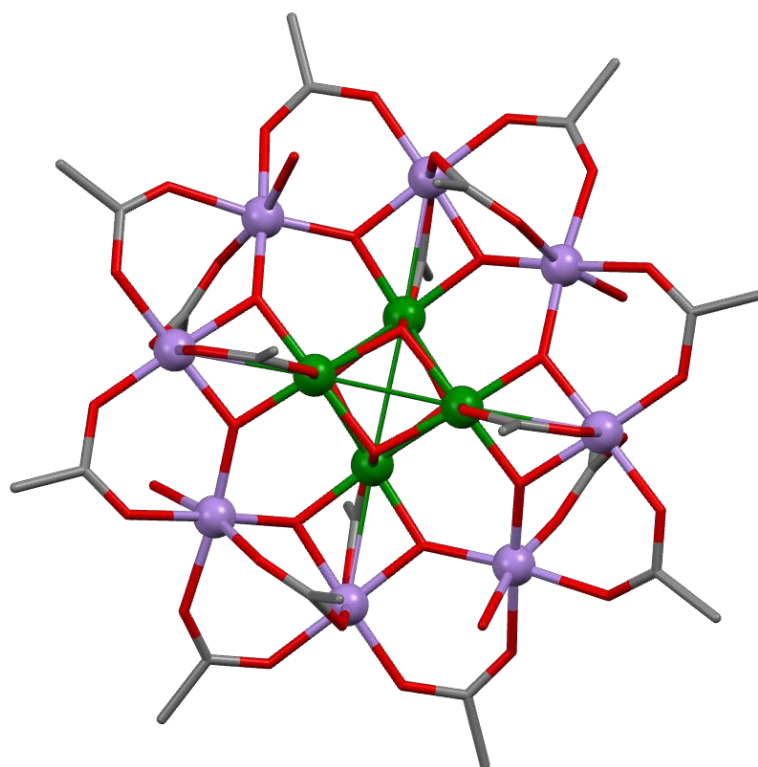


Fig. 1. Molecular structure of Mn₁₂Ac viewed along the crystallographic *c* axis (*S*₄ axis that is the easy axis of magnetization). Atom coloring: violet, Mn^{III}; green, Mn^{IV}; grey, C; red, O, H atoms are omitted for clarity.

In addition to their relevance for information storage and quantum computing, SMMs have been intensively investigated as potential materials for cryogenic magnetic refrigeration based on the magnetocaloric effect (MCE) [12-30]. The conventional MCE relies on the entropy change achieved during isothermal demagnetization process and temperature change occurring in course of adiabatic demagnetization process. Theoretical and experimental studies indicate that an ideal molecular refrigerant should possess a large spin ground state combined with minimal magnetic anisotropy, thereby maximizing the magnetic entropy change upon demagnetization [23,25,28]. An exception to this general trend is the rotational magnetocaloric effect (RMCE) [31, 32], in which the magnetization and demagnetization are achieved by mechanical rotations of the sample in a constant external magnetic field, with the effect being favored by magnetic anisotropy.

Apart from the RMCE scenario, however, the magnetic anisotropy intrinsic to SMMs such as Mn₁₂Ac is generally considered a hindrance for magnetic refrigeration.



The zero-field splitting (ZFS) of spin levels reduces the magnetic entropy change in the low-temperature regime and thus limits the efficiency of conventional MCE-based cooling cycles. In the present work, we adopt a different theoretical perspective that exploits precisely the feature usually regarded as detrimental, namely, strong magnetic anisotropy, to achieve magnetic cooling. We investigate the nonequilibrium thermal processes occurring in Mn_{12}Ac crystals subjected to fast (sudden) magnetic field quenching. Unlike conventional MCE, which assumes a quasi-static reversible process where the system remains close to thermodynamic equilibrium, the present approach focuses on the regime where the magnetic field sweep rate is significantly exceeds the spin–lattice relaxation rate.

Magneto-thermal effect induced by the fast field quenching was previously studied for 3d-metal-based mononuclear complexes in [33,34] as well as for the exchange coupled clusters in [35, 36]. For the mononuclear complexes, it was shown that the relaxation of the spin system from a nonequilibrium state created by the sudden field change to the new equilibrium state is accompanied by a heat flow from the phonon bath to the spin subsystem provided that the system exhibits easy-axis-type anisotropy. This energy transfer results in a cooling of the crystal lattice.

Under such conditions, the strong easy-axis-type magnetic anisotropy of the Mn_{12}Ac is expected to play a dual constructive role. First, it determines the specific energy level pattern required for the cooling mechanism. Second, it ensures sufficiently long relaxation times at low temperatures, making the “sudden” quenching approximation experimentally feasible. Using a theoretical framework and a purely model treatment recently developed by some of us [33-36], in this article we predict and justify a possibility for the nonequilibrium magnetic cooling effect in Mn_{12} family clusters by considering monocrystalline sample of the prototypical single-molecule magnet Mn_{12}Ac as a representative example.

We demonstrate that fast field quenching can induce absorption of the heat by the spin subsystem and hence significant cooling of the crystal lattice in the Mn_{12}Ac . This nonequilibrium magnetic cooling effect represents a magneto-thermal phenomenon that is quite distinct from the MCE and offers a new perspective on the use of highly anisotropic SMMs in the low-temperature physics.

2. Theoretical approach



We will focus on the low-temperature nonequilibrium thermal processes that are expected in the Mn_{12}Ac upon fast (sudden) magnetic field quenching. The isotropic exchange interaction in this cluster is known to stabilize the ground state with the spin $S = 10$. Since this state is well isolated from the excited states, at low temperatures one can consider the Mn_{12}Ac as a magnetic particle with $S=10$. This is the so-called “giant spin approximation” often used to describe the low-temperature properties of the clusters with strong ferromagnetic exchange. Then, the cluster is approximately described by the following spin-Hamiltonian:

$$\hat{H} = D \left[\hat{S}_Z^2 - \frac{1}{3} S(S+1) \right] + g_{\parallel} \mu_B B_Z \hat{S}_Z. \quad (1)$$

This Hamiltonian, Eq. (1), includes the axial component of the ZFS tensor and Zeeman interaction, where D is the axial ZFS parameter defined for the $S=1$ -state, \hat{S}_Z is the Z -component of the spin operator, g_{\parallel} is the parallel component of \mathbf{g} -tensor, μ_B is the Bohr magneton and B_Z is the magnetic field strength in the Z -direction. We will use the following D and g_{\parallel} values reported for the Mn_{12}Ac : $D = -0.5 \text{ cm}^{-1}$ [4], $g_{\parallel} = 2.05$ [8].

In writing down Eq. (1) we have neglected the higher-order ZFS terms, which are several orders of magnitude weaker than the axial ZFS term in Eq. (1), and are not important for the present consideration. For negative D , which is the case here, the system exhibits easy-axis-type magnetic anisotropy and the possesses magnetization reversal barrier responsible for the SMM properties of the Mn_{12}Ac . We will deal with the single crystal sample, and analyze the case when the magnetic field is directed along the easy axis Z .

The eigenvalues of the Hamiltonian, Eq. (1) are obtained as follows:

$$E_{M_S} = D \left[M_S^2 - \frac{1}{3} S(S+1) \right] + g_{\parallel} \mu_B B_Z M_S, \quad (2)$$

where $-S \leq M_S \leq S$. At $B_z=0$ the energy pattern consists of ten non-Kramers doublets with $M_S = \pm 10, \pm 9 \dots \pm 1$ and one singlet with $M_S = 0$ (highest in energy). In applied magnetic field each doublet is split into two Zeeman sublevels as shown in Fig. 2, in

which the energy of the ground state is regarded to be the reference energy. An important feature of this energy pattern (as will be clear from the subsequent discussion) is that the decrease of the field leads to diminishing all energy gaps separating the ground state from the excited ones.



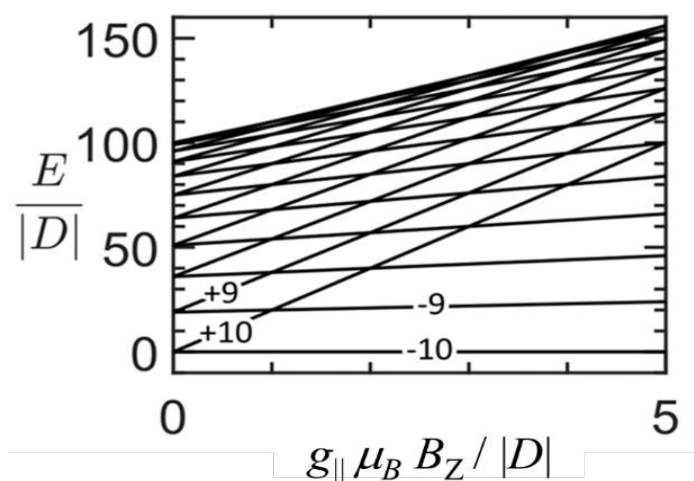


Fig. 2. Energy levels of the $Mn_{12}Ac$ as functions of the axial magnetic field. The M_S -values for the Zeeman sublevels of the ground and the first excited non-Kramers doublets are indicated. The energy of the ground state $|M_S = -10\rangle$ is chosen as the reference energy.

We will analyze the thermal processes arising upon fast (sudden) change of the magnetic field from its initial value B_Z^i to the final value B_Z^f , where $B_Z^f < B_Z^i$. We will consider the case when the sample under study, consisting of the $S=10$ -clusters and the phonon bath, is isolated from the external world with the adiabatic envelope. Under this condition the heat exchange is allowed only between the spin and phonon subsystems within the sample rather than between the sample and the environment. It is also assumed that the field direction remains unchanged in course of switching event. At initial field B_Z^i the $S=10$ -cluster (spin subsystem) is assumed to be in a thermal equilibrium with the phonon bath, and thus it is fully characterized by the set of Boltzmann populations of the spin states, which are the eigenstates of the spin-Hamiltonian, Eq. (1), in which one should set $B_Z = B_Z^i$. The Boltzmann population of the k^{th} state is thus defined as follows:

$$n_k(B_Z^i, T_i) = \frac{\exp\left[-\frac{E_k(B_Z^i)}{k_B T_i}\right]}{\sum_{n=1}^{21} \exp\left[-\frac{E_n(B_Z^i)}{k_B T_i}\right]}, \quad (3)$$



where $E_k(B_Z^i)$ is the k^{th} eigenvalue of the spin-Hamiltonian, Eq. (1), evaluated at $B_Z = B_Z^i$ ($k=1, 2, \dots, 21$), k_B is the Boltzmann constant, and T_i is the initial temperature of the sample. Upon fast changing the field from B_Z^i to B_Z^f , the thermal equilibrium proves to be broken down. Provided that the field change occurs much faster than the spin-lattice relaxation, the populations of the states do not have time to adapt to the new energy pattern corresponding to the field B_Z^f . This means that immediately after the fast field change the populations remain the same as the initial equilibrium populations $n_k(B_Z^i)$, however they cease to be the equilibrium ones. Strictly speaking this statement is valid only because M_S is a good quantum number and hence fast change of the field does not induce any transitions between different Zeeman states.

The fact that the field is quenched suddenly also means that the temperature of the phonon subsystem has no time to change and hence immediately after the field change the temperature of the phonon bath proves to be the same as at the beginning of the process, i. e. it is equal to T_i . Then, the molar internal energy the complex acquired immediately after the field change is thus expressed in terms of the following sum of the products of eigenvalues $E_k(B_Z^f)$ of the spin-Hamiltonian, Eq. (1), evaluated at the final field $B_Z = B_{Zf}$ and the initial equilibrium populations $n_k(B_Z^i)$:

$$U(B_Z^i, B_Z^f, T_i) = N_A \sum_{k=1}^{21} E_k(B_Z^f) n_k(B_Z^i, T_i). \quad (4)$$

where N_A is the Avogadro constant.

The second stage of the considered nonequilibrium magnetothermal process is a relaxation of the system to the new (final) equilibrium state. During this stage the spin and phonon subsystems exchange the heat in order to reach equilibrium. Since the sample (spin subsystem + phonon subsystem) is isolated from the environment, the relaxation should result in the temperature change $\Delta T = T_f - T_i$ when T_f is the final temperature established in the sample as a result of relaxation. The final equilibrium state is characterized by the set of Boltzmann populations

$$n_k(B_Z^f, T_f) = \frac{\exp\left[-\frac{E_k(B_Z^f)}{k_B T_f}\right]}{\sum_{n=1}^{21} \exp\left[-\frac{E_n(B_Z^f)}{k_B T_f}\right]}, \quad (5)$$

and the molar internal energy



$$U'(B_Z^f, T_f) = N_A \sum_{k=1}^{21} E_k(B_Z^f) n_k(B_Z^f, T_f). \quad (6)$$

View Article Online
DOI: 10.1039/D6DT00503A

In the considered case when the sample is isolated from the environment, one can write down the following heat-balance equation:

$$U'(B_Z^f, T_f) - U(B_Z^i, B_Z^f, T_i) + \int_{T_i}^{T_f} C_{ph} dT = 0, \quad (7)$$

where C_{ph} is the heat capacity for the phonons. For the low temperature range, we are interested in here, the Debye law seems to be a good approximation:

$$C_{ph} = \frac{12}{5} \pi^4 N_A k_B (T/\theta_D)^3, \quad (8)$$

where θ_D is the Debye temperature. For Mn_{12}Ac $\theta_D = 40.9$ K [9]. Note that the number of oscillating units in Eq. (8) is assumed to be equal to the number of spins in Eqs. (4) and (6), which seems to be a reasonable assumption as applied to the long-wave acoustic phonons participating in Debye phonon heat capacity, when each Mn_{12}Ac cluster can be imagined to be oscillating as a whole. By using Eqs. (4) and (6) and performing integration one can present Eq. (7) in the following final form

$$\sum_{k=1}^{21} E_k(B_Z^f) [n_k(B_Z^f, T_f) - n_k(B_Z^i, B_Z^f, T_i)] + \frac{3\pi^4 k_B}{5\theta_D^3} (T_f^4 - T_i^4) = 0. \quad (9)$$

To find the final temperature T_f (or, alternatively, the temperature change $\Delta T = T_f - T_i$) as a function of the initial temperature T_i and the initial and final magnetic fields B_Z^i and B_Z^f , one should solve Eq. (9). However, some preliminary conclusions concerning the sign of the thermal effect (heating *versus* cooling) can be derived even prior to solving this equation, just based on the analysis of the field dependencies of the energy levels shown in Fig. 1. Stabilization of the excited states upon field decrease leads to the underpopulation of the excited states immediately after fast field change, which means that in order to come to the equilibrium state the heat should pass from the phonon bath to the spin subsystem in course of relaxation, which should lead to diminishing of the temperature. Such nonequilibrium magnetic cooling effect has already been mentioned for much simpler system with $D < 0$ representing mononuclear paramagnetic complex having $S=1$ (e. g., Ni(II) complex) [33,34]. Such kind of magnetothermal behavior seems to be a common feature of all magnetic molecules with easy-axis-type anisotropy. Below we will support the conclusion about the possibility



of low-temperature magnetic cooling in $Mn_{12}Ac$ based on the numerical solution of Eq. (9). View Article Online
DOI: 10.1039/D6DT00503A

3. Results and discussion

The theoretical framework described above is valid under the condition of fast (“sudden”) magnetic field variation. This implies that during the field quenching process the spin and phonon subsystems do not have sufficient time to exchange heat. Quantitatively, this requires that the field switching time t_q be significantly shorter than the spin-relaxation time τ . In the present analysis it is assumed that t_q is one order of magnitude shorter than τ . We consider the field decrease of 1 T as an upper limit of the change of the field. Then, by considering the sweep rate of about 10 T/s (a relatively fast but experimentally achievable rate), we estimate the upper limit of the quenching times as $t_q^{max} = 0.1$ s. Then, to meet the condition the relaxation time should be no less than 1s. This restriction defines the temperature range where the sudden field quenching approach is applicable.

It is important to emphasize that Mn_{12} clusters exhibit exceptionally slow spin dynamics at low temperatures, with relaxation times spanning many orders of magnitude. For the thermally activated regime that excludes extremely low temperatures (approximately $T \gtrsim 3-5$ K for many compounds), the temperature dependence of the relaxation time is described by the Arrhenius law:

$$\tau = \tau_0 \exp\left(\frac{U_b}{T}\right), \quad (10)$$

where τ_0 is the pre-exponential factor, and U_b is the magnetization reversal barrier. For a representative example of $Mn_{12}Ac$ these parameters are known to be: $\tau_0 = 2.1 \cdot 10^{-7}$ s and $U_b = 70.3$ K [4]. These values are typical for a broad class of Mn_{12} derivatives, as discussed above. In order to justify the use of $Mn_{12}Ac$ as a representative example, it is instructive to note that closely related members of the $[Mn_{12}O_{12}(RCOO)_{16}(H_2O)_4]$ family exhibit Arrhenius parameters of comparable magnitude. Similar barrier heights have been reported for several carboxylate-substituted derivatives with $S = 10$ ground state and axial anisotropy of the Mn_{12} core. More generally, high-frequency EPR and AC susceptibility studies across a broad series of Mn_{12} derivatives indicate that the dominant relaxation barrier in the thermally activated regime typically lies between ~ 50 and 70 K, with pre-exponential factors commonly in the range $10^{-8}-10^{-6}$ s. [1] For example, Mn_{12} complexes incorporating naphthalene-carboxylate ligands exhibit



effective barriers in the range $U_b=53\text{--}61$ K, as determined from AC susceptibility measurements in the Arrhenius regime.[37]. These values remain of the same order of magnitude as for Mn_{12}Ac , despite the substantially bulkier peripheral ligands. Likewise, dichloroacetate derivatives such as $(\text{PPh}_4)_2[\text{Mn}_{12}\text{O}_{12}(\text{O}_2\text{CCHCl}_2)_{16}(\text{H}_2\text{O})_4]$ display thermally activated relaxation with effective barriers in the range $U_b\approx 18\text{--}32$ K, depending on crystal form and solvation [38]. Finally, studies on Mn_{12} -Stearate $[\text{Mn}_{12}\text{O}_{12}(\text{CH}_3(\text{CH}_2)_{16}\text{CO}_2)_{11}(\text{CH}_3\text{CO}_2)_5(\text{H}_2\text{O})_4]$ show for bulk the activation energy U_b in the range of 60 K to 62 K and τ_0 that is typically around 10^{-8} to 10^{-4} s, demonstrating that changing the carboxylate ligand can modulate the relaxation behavior [39]. Thus, while ligand substitution, solvation, and crystal packing can modulate the effective barrier and relaxation prefactor, the Arrhenius parameters of Mn_{12}Ac may reasonably be regarded as representative for the high-temperature over-barrier relaxation regime in this family. The estimates given so far provide a good justification for the sudden-quench approximation adopted in the present analysis.

Figure 3 shows the temperature dependence of the relaxation time for the Mn_{12}Ac . To fulfill the condition of fast quenching the relaxation times should satisfy the inequality $\tau \geq 1$ s. This defines the maximal temperature at which the fast field quenching approach is still valid as $T_{max} \approx 4.6$ K. Below we will show that the key features of the magnetothermal behavior of the Mn_{12}Ac fit well into this allowed temperature range.

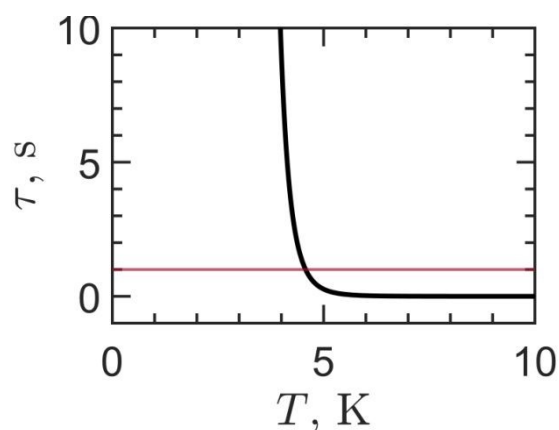


Fig 3. Temperature dependence of the relaxation time for Mn_{12}Ac . Red line marks $\tau = 1$ s, which is the minimal relaxation time for which the fast field switching approach is applicable.



Figure 4 shows the dependencies of ΔT on the initial temperature T_i evaluated for the Mn_{12}Ac at two values of the initial field B_Z^i and different values of the final field B_Z^f by solving the heat-balance equation, Eq. (9). One can see that the temperature change ΔT is always negative, which means that sudden magnetic field quenching causes the system cooling in accordance with the above qualitative arguments according to which sudden decrease of the field produces underpopulations of the excited spin-states of the Mn_{12}Ac , which gives rise to the heat flow directed from phonons to the spin subsystem. In the low-temperature limit ΔT tends to zero, because in this limit only the ground state is populated. Also ΔT goes to zero in the high temperature limit both because the phonon heat capacity rapidly increases with the increase of the temperature and due to the fact, that in the high-temperature limit all states are equally populated, which precludes from the heat exchange between the two subsystems. In between these two limits, the function $\Delta T(T_i)$ passes through the minimum corresponding to the most efficient cooling. It is seen from the comparison of the plots in Figs. 4a and 4b that by increasing the initial magnetic field one can reinforce the cooling effect, however at both initial fields this effect remains rather weak provided that the field is switched off completely (curves with $B_Z^f = 0$ T in Figs. 4a and 4b). The effect can be several orders of magnitude enhanced if the field quenching is incomplete (compare the minimal ΔT values calculated with $B_Z^f = 0$ T

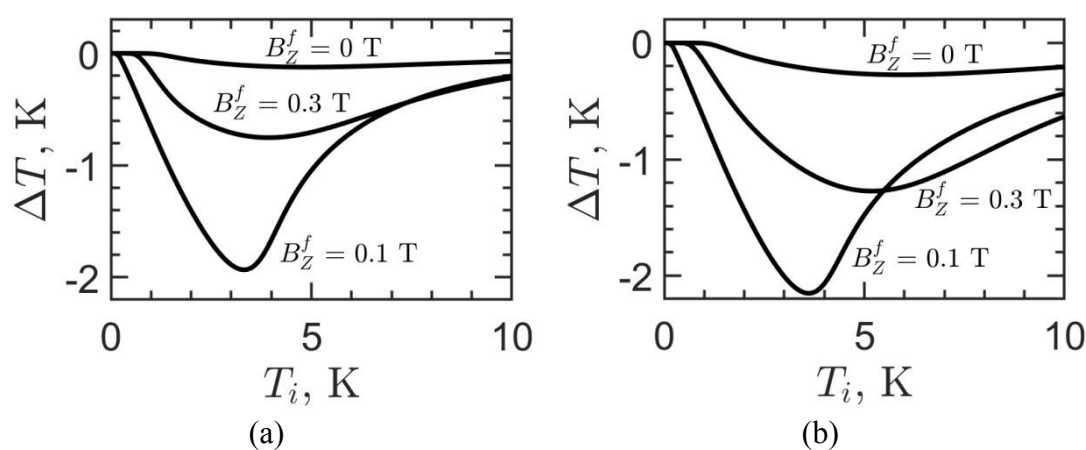


Fig. 4. Dependencies of ΔT on the initial temperature T_i evaluated at $B_Z^i = 0.5$ T (a) and 1 T (b) and different B_Z^f values shown in the plots.



and 0.1 T). Note that at weak final fields $(\Delta T)_{min}$ decreases with the increase of B_Z^f and then starts to decrease when the final field becomes strong enough, as can be seen from comparing the curves evaluated at $B_Z^f = 0.1$ T and 0.3 T.

To get more details about the effects of the initial and final fields on the magnetic cooling effect, we have plotted in Fig. 5 the dependencies of the minimal temperature change $(\Delta T)_{min}$ and the initial temperature $(T_i)_{min}$ at which the minimum of the temperature change is reached on B_Z^f calculated for the two B_Z^i values. In these plots B_Z^f varies from 0 to B_Z^i . It follows from Fig. 5 that cooling effect is stronger at higher initial field. It is also seen that both $(T_i)_{min}$ and $(\Delta T)_{min}$ depend on B_Z^f non-monotonically. Very small deviation of B_Z^f from zero leads to the abrupt decrease of

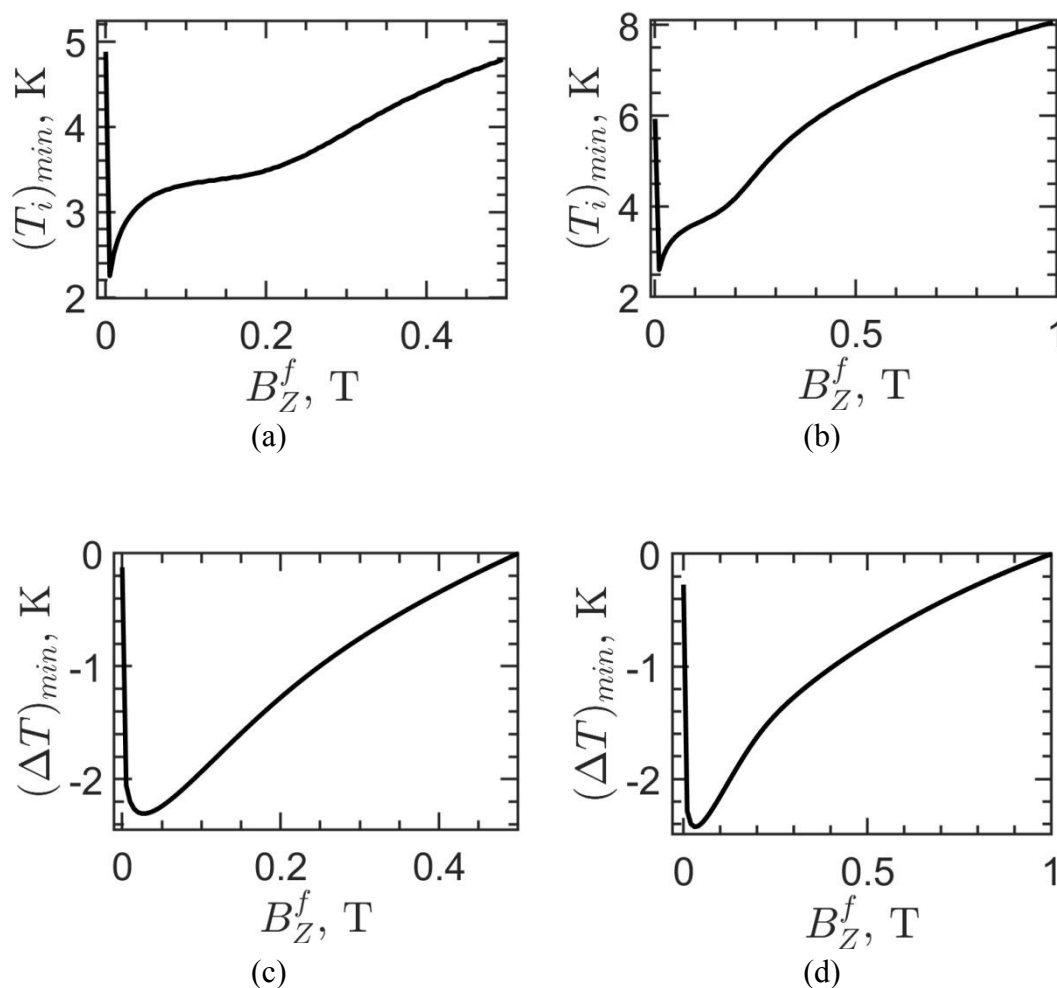


Fig. 5. Dependencies of $(T_i)_{min}$ (a, b) and $(\Delta T)_{min}$ (c, d) on the final magnetic field B_Z^f evaluated at the following two values of the initial field: $B_Z^i = 0.5$ T (a, c),



and $B_Z^i = 1$ T(b, d).

the temperature ensuring maximal cooling (Figs. 5a and 5b) and also to the pronounced enhancement of the cooling effect (Figs. 5c and 5d). In contrast, for stronger deviation of B_Z^f from zero the increase of B_Z^f gives rise to gradual increasing of $(T_i)_{min}$ and $(\Delta T)_{min}$ values.

The main conclusion, which can be drawn by inspecting Figs. 4 and 5 is that for the $Mn_{12}Ac$ one can predict a pronounced magnetic cooling effect of a few K in the temperature range $T < 4.6$ K, at which the condition of suddenness of field quenching is fulfilled at quite achievable sweep rate of the field of about 10 T/s.

At this stage it is appropriate to compare the non-equilibrium magnetothermal effect under study with the conventional MCE which occurs under the condition that magnetic field change occurs so slowly that thermal equilibrium is maintained at any moment in time during the process of changing the field. Then the temperature change in the adiabatic conditions can be evaluated based on the fact that the adiabatic process is isentropic, and so $S_{tot}(B_Z^f, T_f) = S_{tot}(B_Z^i, T_i)$.

$$(11)$$

In this equation the total entropy of the system is defined as follows:

$$S_{tot}(B_Z, T) = S_m(B_Z, T) + S_{ph}(T), \quad (12)$$

where

$$S_m(B_Z, T) = -N_A k_B \sum_k n_k(B_Z, T) \ln[n_k(B_Z, T)] \quad (13)$$

is the entropy of the spin subsystem, and

$$S_{ph}(T) = \frac{4\pi^4 N_A k_B}{5} (T/\theta_D)^3 \quad (14)$$

is the entropy of the phonon subsystem defined within the Debye model. By solving Eq. (12) one can determine the temperature change ΔT occurring upon adiabatic demagnetization.

In Figure 6 one can see the comparison of the temperature dependence of ΔT evaluated for the non-equilibrium process with that found for quasistatic process (i. e. for conventional MCE) by solving Eq. (11). It is seen that MCE and non-equilibrium effect provide comparable temperature changes of several K at low temperatures. Although MCE proves to be slightly stronger than the non-equilibrium magnetothermal effect, a significant advantage of the latter effect is that at slow relaxation exhibited by



Mn₁₂Ac it allows much faster temperature change, which can be important in cryogenic applications.

View Article Online
DOI: 10.1039/D6DT00503A

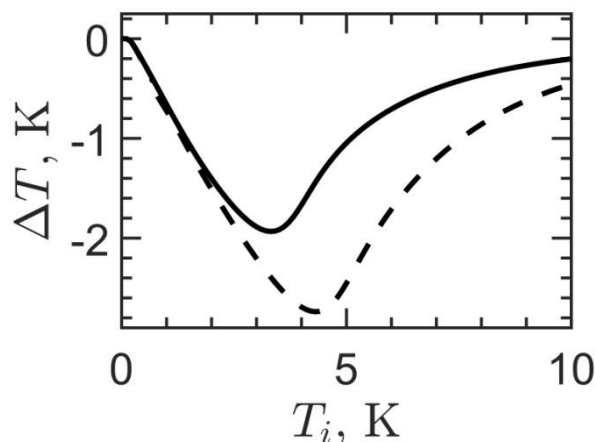


Fig. 6. The temperature change ΔT evaluated as function of the initial temperature T_i at $B_{zi} = 0.5$ T and $B_{zf} = 0.1$ T for the non-equilibrium process (solid line) and quasistatic process occurring in MCE (dashed line).

It is worth to make some remarks regarding experimental feasibility and possible realization of the cooling mechanism proposed in this article. The non-equilibrium cooling mechanism is based on three key conditions: (i) sufficiently fast magnetic field quenching, (ii) slow enough (under the conditions specified so far) spin-lattice relaxation, and (iii) a rather good thermal isolation of the sample. All three requirements can be realistically fulfilled experimentally on Mn₁₂-based SMMs.

First, magnetic field sweep rates on the order of 1–10 T/s are experimentally accessible. Such rates have been achieved in pulsed-field experimental facilities and have been employed in the studies of molecular nanomagnets and particularly their magnetization dynamics [8, 40, 41]. Fast local magnetic field variations can be realized using microcoil or micro-SQUID-based techniques developed for studies of nanomagnets and SMMs [40,41, 42].

Thus, for the practical implementation of fast quenching of magnetic field, no new specific experimental techniques are required [43,44].

Second, the required separation of time scales ($\tau_{\text{switch}} \ll \tau$) is naturally fulfilled in Mn₁₂ systems in the low-temperature regime. As discussed above, the relaxation times exceed 1s typically below 4.5 K and increase rapidly upon further cooling,



reaching values of many seconds or even longer in the magnetic blocking regime. These time scales are well established from AC susceptibility and magnetization relaxation measurements [45,8] with the use of the experimental set up as previously mentioned.

Third, detection of the predicted temperature changes, of the order of several Kelvin, can in principle be achieved using sensitive fast-response thermometry combined with microcalorimetric techniques. Experimental approaches of this type are routinely employed in studies of magnetocaloric effects in molecular materials [4, 16]. Realization of the proposed protocol would require weak thermal exchange between the sample and environment in order to fulfil the adiabatic conditions on the time scale of the field sweep and subsequent relaxation. Although achieving ideal adiabatic insulation is the most challenging experimental part of the problem, in practice such conditions can be achieved using traditional low-temperature calorimetric methods. Typically, the sample is mounted on a platform connected to the thermostat via an insulating thermal connection (including, for example, thin insulating supports or low-thermal-conductivity wires) and placed in a vacuum environment to suppress convective heat dissipation. Under these conditions, that can be treated as quasi-adiabatic on the experimental time scale, the heat exchange occurs mainly between the spin and phonon subsystems.

Along with the common methods in molecular magnetism, some advanced experimental techniques that could be useful in the problem of non-equilibrium low-temperature magnetic cooling effect are also worth mentioning. Nuclear Magnetic Resonance (NMR) is an excellent probe of local spin dynamics and has been extensively used to study Mn_{12}Ac [46]. The method monitors the relaxation of nuclear spins ^1H or ^{55}Mn which are coupled to the electronic spins of the Mn_{12}Ac cluster. By measuring time dependence of the relaxation time T_1 after field quench, one can detect the evolution of the spin temperature. Muon Spin Rotation/Relaxation (μSR) [46] technique seems to be promising because it is very sensitive to slow spin dynamics and has been successfully used in Mn_{12}Ac for studying spin relaxation. Less common, but effective, are optical methods focused on the study of spin dynamics such as magneto-optical methods (magnetic circular dichroism and Faraday effect) which has already been applied to Mn_{12}Ac .

4. Conclusions

In this article we have presented a theoretical analysis of the nonequilibrium magnetothermal processes which can be expected in single crystal sample of SMM



Mn₁₂Ac upon fast (sudden) quenching of the external magnetic field applied along the easy axis of magnetization. We demonstrate that such rapid field variation can induce cooling of the sample. In contrast to the conventional MCE, where magnetic anisotropy is generally considered as a detrimental factor hindering efficient magnetic cooling, the strong easy-axis anisotropy of Mn₁₂Ac is the key prerequisite for the implementation of the proposed cooling mechanism.

The cooling effect originates from the mismatch between the initial spin populations, which remain the same during the fast field change, and the new energy level structure formed by the final magnetic field. The subsequent relaxation of the spin system toward equilibrium requires energy absorption from the phonon bath, leading to a decrease in the lattice temperature under adiabatic conditions.

Numerical analysis based on solving the heat-balance equation reveals several important features of this process. First, the easy-axis-type anisotropy in Mn₁₂Ac determines the direction of a heat flow from the lattice subsystem to the spin-subsystem during the relaxation after sudden field switching, which leads to the lattice cooling. The significant cooling effect up to several Kelvin is predicted, confirming the potential of the Mn₁₂Ac as a low-temperature refrigerant in this specific dynamic mode. Second, a non-trivial dependence of the final temperature on the final magnetic field has been deduced. Particularly, it has been found that incomplete field quenching can be more efficient than switching the field off completely. This can be attributed to the optimization of energy gaps between the ground and excited states, which maximizes the heat intake by the spin system.

The considered approach is applicable in the low-temperature range (below approximately 4.6 K for Mn₁₂Ac), where the spin-lattice relaxation time is sufficiently long ($\tau > 1$ s) to satisfy the condition of sudden field quenching at experimentally achievable sweep rates of ~ 10 T/s. The presented arguments regarding the experimental feasibility and possible implementation of the cooling mechanism on single-molecule magnets based on Mn₁₂ show that the proposed scheme is quite realistic. We hope that the present predictions could stimulate specifically oriented experimental studies of the fast-field magnetothermal effects in SMMs.

Overall, the present study provides a new perspective on the utilization of highly anisotropic molecular clusters in cryogenic applications. We also show that by shifting from quasi-static thermodynamic cycles to non-equilibrium dynamic protocols, SMMs

View Article Online
DOI: 10.1039/D6DT00503A

Dalton Transactions Accepted Manuscript



with high relaxation barriers can serve as effective cooling agents, complementing the traditional low-anisotropy molecular refrigerants.

Conflicts of interest

There are no conflicts to declare.

Acknowledgements

A. P., V. B., D. K. and S. A. acknowledge financial support from the Russian Science Foundation (Project No. 25-13-00010).

References

1. Sessoli, R.; Gatteschi, D.; Caneschi, A.; Novak, M. A. Magnetic bistability in a metal-ion cluster. *Nature* **1993**, 365, 141-143.
2. Gatteschi, D.; Sessoli, R.; Villain, J., *Molecular Nanomagnets*, Oxford University Press, NY, **2006**.
3. Christou, G.; Stamatatos, T. C.; Foguet-Albiol, D., Single-molecule magnets: a molecular approach to nanoscale magnetic materials, *Coordination Chemistry Reviews* **2008**, 252, 1857–1877.
4. Affronte, M. in: *Molecular nanomagnets and related phenomena (Structure and Bonding, Vol. 164)*. **2015**, S. Gao (Ed.). Berlin: Springer.
5. Mannini, M.; Pineider, F.; Sainctavit, P.; Danieli, C.; Otero, E.; Sciancalepore, C.; Sessoli, R. Magnetic memory of a single-molecule quantum magnet wired to a gold surface. *Nature materials* **2009**, 8, 194-197.
6. Moreno-Pineda, E.; Wernsdorfer, W. Measuring molecular magnets for quantum technologies. *Nature Reviews Physics* **2021**, 3, 645-659.
7. Caneschi, A.; Gatteschi, D.; Sessoli, R.; Barra, A.-L.; Brunel, L. C.; Guillot, M. Alternating current susceptibility, high field magnetization, and millimeter band EPR evidence for a ground $S=10$ state in $[\text{Mn}_{12}\text{O}_{12}(\text{CH}_3\text{COO})_{16}(\text{H}_2\text{O})_4] \cdot 2\text{CH}_3\text{COOH} \cdot 4\text{H}_2\text{O}$. *J. Am. Chem. Soc.* **1991**, 113, 5873-5874.
8. Perenboom, J. A. A. J.; Brooks, J. S.; Hill, S.; Hathaway, T.; Dalal, N. S. Relaxation of the magnetization of Mn₁₂ acetate. *Phys. Rev. B* **1998**, 58, 330.
9. Fominaya, F.; Villain, J.; Fournier, T.; Gandit, P.; Chaussy, J.; Fort, A.; Caneschi, A. Magnetic-field-dependent thermodynamics of Mn₁₂-acetate single crystals at low temperatures. *Phys. Rev. B* **1999**, 59, 519.
10. Eppley, H.J., Tsai, H.-L., Devries, N., Folting, K., Christou, G. Hendrickson, D.N. (1995). *J. Am. Chem. Soc.* 117, 301.



11. Aubin, S.M.J., Sun, Z.M., Eppley, H.J., Rumberger, E.M., Guzei, I.A., Foltyn, K., Gantzel, P.K., Rheingold, A.L., Christou, G., Hendrickson, D.N. (2001). *Inorg. Chem.* **40**, 2127. View Article Online
DOI: 10.1039/D00503A
12. Torres, F.; Hernández, J. M.; Bohigas, X.; Tejada, J. Giant and time-dependent magnetocaloric effect in high-spin molecular magnets. *Appl. Phys. Lett.* **2000**, *77*, 3248-3250.
13. Spichkin, Y.I.; Zvezdin, A.K.; Gubin, S.P.; Mischenko, A.S.; Tishin, A.M. Magnetic molecular clusters as promising materials for refrigeration in low-temperature regions. *J. Phys. D Appl. Phys.* **2001**, *34*, 1162–1166.
14. Affronte, M.; Ghirri, A.; Carretta, S.; Amoretti, G.; Piligkos, S.; Timco, G. A.; Winpenny, R.E.P. Engineering molecular rings for magnetocaloric effect. *Appl. Phys. Lett.* **2004**, *84*, 3468–3470.
15. Evangelisti, M.; Candini, A.; Ghirri, A.; Affronte, M. Spin-enhanced magnetocaloric effect in molecular nanomagnets. *Appl. Phys. Lett.* **2005**, *87*, 072504.
16. Evangelisti, M.; Luis, F.; de Jongh, L.J.; Affronte, M. Magnetothermal properties of molecule-based materials. *J. Mater. Chem.* **2006**, *16*, 2534–2549.
17. Manoli, M.; Johnstone, R.D.L.; Parsons, S.; Murrie, M.; Affronte, M.; Evangelisti, M.; Brechin, E.K. A Ferromagnetic Mixed-Valent Mn Supertetrahedron: Towards Low-Temperature Magnetic Refrigeration with Molecular Clusters. *Angew. Chem. Int. Ed.* **2007**, *46*, 4456–4460.
18. Manoli, M.; Collins, A.; Parsons, S.; Candini, A.; Evangelisti, M.; Brechin, E.K. Mixed-valent Mn supertetrahedra and planar discs as enhanced magnetic coolers. *J. Am. Chem. Soc.* **2008**, *130*, 11129–11139.
19. Evangelisti, M.; Candini, A.; Affronte, M.; Pasca, E.; de Jongh, L.J.; Scott, R.T.W.; Brechin, E.K. Magnetocaloric effect in spin-degenerated molecular nanomagnets. *Phys. Rev. B* **2009**, *79*, 104414.
20. Zheng, Y.-Z.; Evangelisti, M.; Winpenny, R.E.P. Large Magnetocaloric Effect in a Wells–Dawson Type $\{\text{Ni}_6\text{Gd}_6\text{P}_6\}$ Cage. *Angew. Chem. Int. Ed.* **2011**, *50*, 3692–3695.
21. Zheng, Y.-Z.; Evangelisti, M.; Winpenny, R.E.P. Co–Gd phosphonate complexes as magnetic refrigerants. *Chem. Sci.* **2011**, *2*, 99–102.
22. Evangelisti, M.; Roubeau, O.; Palacios, E.; Camon, A.; Hooper, T.N.; Brechin, E.K.; Alonso, J.J. Cryogenic Magnetocaloric Effect in a Ferromagnetic Molecular Dimer. *Angew. Chem. Int. Ed.* **2011**, *50*, 6606–6609.



23. R. Sessoli, Chilling with magnetic molecules. *Angew. Chem., Int. Ed.* **2012**, *51*, 43–45. View Article Online
DOI: 10.1039/D6DT00503A
24. Garlatti, E.; Carretta, S.; Schnack, J.; Amoretti, G.; Santini, P. Theoretical design of molecular magnets for magnetic refrigeration. *Appl. Phys. Lett.* **2013**, *103*, 202410.
25. Bałanda, M.; Pełka, R.; Fitta, M.; Laskowski, Ł.; Laskowska, M. Relaxation and magnetocaloric effect in the Mn₁₂ molecular nanomagnet incorporated into mesoporous silica: comparative study. *RSC Advances* **2016**, *6*, 49179–49186.
26. Zheng, X.Y.; Kong, X.J.; Zheng, Z.; Long, L.S.; Zheng, L.S. High-nuclearity lanthanide-containing clusters as potential molecular magnetic coolers. *Acc. Chem. Res* **2018**, *51*, 517–525.
27. Konieczny, P.; Sas, W.; Czernia, D.; Pacanowska, A.; Fitta, M.; Pełka, R. Magnetic cooling: A molecular perspective. *Dalton Trans.* **2022**, *51*, 12762–12780.
28. Raza, A.; Perfetti, M. Electronic structure and magnetic anisotropy design of functional metal complexes. *Coord. Chem. Rev.* **2023**, *490*, 215213.
29. Agapaki, E.; Charkiolakis, E.K.; Nichol, G.S.; Gracia, D.; Evangelisti, M.; Brechin, E.K. Magnetocaloric effect in a high-spin ferromagnetic molecular cluster. *Front. Chem.* **2024**, *12*, 1494609.
30. Fang, M.; Dang, Y.; Ma, M.; Shao, Y.; Luan, Y.; Tang, Z.; Ma, Y.; Shi, B. Two tetranuclear lanthanide complexes respectively featuring magnetocaloric effect and slow magnetization relaxation. *J. Mol. Struct.* **2025**, *1334*, 141750.
31. Beckmann, C.; Ehrens, J.; Schnack, J. Rotational magnetocaloric effect of anisotropic giant-spin molecular magnets. *J. Magn. Magn. Mater.* **2019**, *482*, 113–119.
32. Konieczny, P.; Czernia, D.; Kajiwar, T. Rotating magnetocaloric effect in highly anisotropic Tb^{III} and Dy^{III} single molecular magnets. *Sci. Rep.* **2022**, *12*, 16601.
33. Palii, A.; Tsukerblat, B. Thermal processes in anisotropic metal complexes induced by non-adiabatic switching of magnetic field. *Dalton Trans.* **2024**, *53*, 9161–9270.
34. Palii, A.; Belonovich, V.; Tsukerblat, B. Refrigeration in adiabatically confined anisotropic transition metal complexes induced by sudden magnetic field quenching. *Magnetochemistry* **2025**, *11*, 69.
35. Palii, A.; Belonovich, V.; Aldoshin, S.; Tsukerblat, B. Modelling thermal effects in Heisenberg dimers initiated by fast magnetic field switching off. *J. Chem. Phys.* **2025**, *163*, 024130.



36. Palii, A.; Belonovich, V.; Aldoshin, S.; Tsukerblat, B. Non-equilibrium magnetothermal effects in Ising dimers: Relevance to the problem of low-temperature magnetic refrigeration. *Phys. Chem. Chem. Phys.* **2025**, *27*, 16607–16619. View Article Online
DOI: 10.1039/D6DT00503A
37. Bian, G.-Q.; Kuroda-Sowa, T.; Nogami, T.; Sugimoto, K.; Maekawa, M.; Munakata, M.; Miyasaka, H.; Yamashita, M. Syntheses, Crystal structure, and magnetic properties of Mn₁₂ single-molecule magnets with naphthalenecarboxylate bridges, [Mn₁₂O₁₂(O₂CC₁₀H₇)₁₆(H₂O)₄] and their tetraphenylphosphonium salts, *Bull. Chem. Soc. Jpn.*, **2005**, *78*, 1032–1037.
38. Soler, M.; Wernsdorfer, W.; Abboud, K. A.; Huffman, J. C.; Davidson, E. R.; Hendrickson, D. N.; Christou, G. Single-molecule magnets: two-electron reduced version of a Mn₁₂ complex and environmental influences on the magnetization relaxation of (PPh₄)₂[Mn₁₂O₁₂(O₂CCHCl₂)₁₆(H₂O)₄], *J. Am. Chem. Soc.*, **2003**, *125*, 3576–3588.
39. Verma, S.; Verma, A.; Srivatsava, A. K.; Gupta, A.; Singh, S. P.; Singh, P., Structural and magnetic properties of Mn₁₂-Stearate nanomagnets, *Mater. Chem. Phys.*, **2016**, *177*, 140-146.
40. Wernsdorfer, W. From micro- to nano-SQUIDS: applications to nanomagnetism, *Supercond. Sci. Technol.* 2009, *22*, 064013.
41. Friedman J. R.; Sarachik, M. P.; Tejada J.; Ziolo, R. Macroscopic Measurement of Resonant Magnetization Tunneling in High-Spin Molecules, *Phys. Rev. Lett.* **1996**, *76*, 3830-3833.
42. Thomas, L.; Lioni, F.; Ballou, R.; Gatteschi, D.; Sessoli, R.; Barbara, B. Macroscopic quantum tunnelling of magnetization in a single crystal of nanomagnets, *Nature*, 1996, *383*, 145–147.
43. Paulsen, C.; Jackson, M. J.; Lhotel, E.; Canals, D.; Prabhakaran, K.; Matsuhira, S. R.; Giblin, S. T.; Bramwell, S. T. Far from equilibrium monopole dynamics in spin ice, *Nature Physics*, **2014**, *10*, 135–139.
44. Jackson, M. J.; Lhotel, E.; Giblin, S. R.; Bramwell, S. T.; Prabhakaran, D.; Matsuhira, K.; Hiroi, Z.; Yu, Q.; Paulsen, C. Dynamic behavior of magnetic avalanches in the spin-ice compound Dy₂Ti₂O₇, *Phys. Rev. B*, **2014**, *90*, 064427
45. Caneschi, A.; Gatteschi, D.; Sessoli, R. Alternating current susceptibility, high field magnetization, and millimeter band EPR Evidence for a Ground S = 10



State in $[\text{Mn}_{12}\text{O}_{12}(\text{CH}_3\text{COO})_{16}(\text{H}_2\text{O})_4]\cdot 2\text{CH}_3\text{COOH}\cdot 4\text{H}_2\text{O}$, *J. Am. Chem. Soc.* View Article Online
DOI: 10.1039/D6DT00503A 1991, 113, 5873-5874.

46. Borsa F.; Furukawa Y.; Lascialfari, A.; Review of NMR and μSR studies in the molecular nanomagnet Mn₁₂-ac, *Inorg. Chim. Acta* , **2008**, 361, 3777-3784.



Data availability statement

View Article Online
DOI: 10.1039/D6DT00503A

Numerical data and Wolfram's Mathematica programs for calculation of the thermocaloric effect characteristics are available from corresponding authors upon request.

